

Localized Spins on Graphene

P. S. Cornaglia, Gonzalo Usaj, and C. A. Balseiro

*Centro Atómico Bariloche and Instituto Balseiro, CNEA, 8400 Bariloche, Argentina and
Consejo Nacional de Investigaciones Científicas y Técnicas (CONICET), Argentina*

(Dated: September 5, 2018)

The problem of a magnetic impurity, atomic or molecular, absorbed on top of a carbon atom in otherwise clean graphene is studied using the numerical renormalization group. The spectral, thermodynamic, and scattering properties of the impurity are described in detail. In the presence of a small magnetic field, the low energy electronic features of graphene make possible to inject spin polarized currents through the impurity using a scanning tunneling microscope (STM). Furthermore, the impurity scattering becomes strongly spin dependent and for a finite impurity concentration it leads to spin polarized bulk currents and a large magnetoresistance. In gated graphene the impurity spin is Kondo screened at low temperatures. However, at temperatures larger than the Kondo temperature, the anomalous magnetotransport properties are recovered.

PACS numbers: 73.20.Hb, 73.20.-r, 73.23.-b, 81.05.Uw, 99.10.Fg

Graphene is a two dimensional material made of carbon atoms arranged in a hexagonal lattice. Its structural stability and unusual electronic properties [1, 2, 3, 4, 5, 6] make it an excellent candidate for technological applications. The low energy electronic structure corresponds to massless, chiral, fermionic quasiparticles described by the Dirac equation. Graphene is a semimetal that can be globally or locally doped with electrons or holes using gate electrodes. These characteristics triggered an intense activity that ranges from the search of new devices to the study of new scenarios for Dirac fermions [5, 6]. Important advances have been made in the preparation and characterization of this material. One of the ongoing goals is to incorporate spintronic effects in graphene and this requires the development of simple tools for the manipulation and control of the carrier's spins. There are already some advances in this direction like the injection of a spin polarized current from ferromagnetic electrodes [7, 8]. There are also some theoretical proposals involving the use of edge states to transport spin polarized currents [9, 10]. Despite the intense activity in the area, the properties of graphene with magnetic impurities, atoms or molecules, have received less attention. Previous works using mean field approaches already pointed out the unusual behavior of some properties as well as the possibility of controlling the magnetic structure of the impurity with electric fields [11, 12, 13]. The magnetic screening of an impurity spin, the Kondo effect, in systems with graphenelike pseudogaps has also been analyzed by several authors [14, 15, 16].

In this work we address the problem of graphene with magnetic impurities and show that the peculiar electronic properties of this system lead to some interesting new effects. In particular, we show the potential use of these impurities to inject and generate spin polarized currents. When an impurity is adsorbed on top of a carbon atom, the impurity levels acquire a finite lifetime, that is, the spectral function shows broad peaks. In the undoped

case, despite of the broadening of its levels the impurity behaves as a free spin at low temperatures and we show that with a small magnetic field, such that the Zeeman energy is larger than the thermal energy $k_B T$, a *non-magnetic* STM tip can be used to inject spin polarized electrons with an extraordinary efficiency. In this regime we also show that the bulk transport properties present interesting features: in the absence of electron-hole symmetry and with a finite impurity concentration there is a large magnetoresistance and the transport current is spin polarized. Conversely, a magnetic impurity in doped graphene leads to the Kondo effect. While in general the Kondo temperature T_K is small due to the small density of states at the Fermi energy of graphene, in some cases it could be well above the experimentally accessible limits.

Our starting point is the Anderson model describing an impurity with a single orbital of energy ε_d and Coulomb repulsion U hybridized with the conduction electron states with a matrix element V_{hyb} . The Hamiltonian of the system is then $H = H_{\text{imp}} + H_{\text{graph}} + H_{\text{hyb}}$, where the first term is given by

$$H_{\text{imp}} = \sum_{\sigma} (\varepsilon_d - \sigma \mu B) d_{\sigma}^{\dagger} d_{\sigma} + U d_{\uparrow}^{\dagger} d_{\uparrow} d_{\downarrow}^{\dagger} d_{\downarrow}. \quad (1)$$

Here d_{σ}^{\dagger} creates an electron with spin σ at the impurity state and μB is the Zeeman energy shift due to an external in-plane magnetic field B . The Hamiltonian of the graphene layer is

$$H_{\text{graph}} = -t \sum_{\mathbf{k}, \sigma} \phi(\mathbf{k}) a_{\mathbf{k}\sigma}^{\dagger} b_{\mathbf{k}\sigma} + \phi^*(\mathbf{k}) b_{\mathbf{k}\sigma}^{\dagger} a_{\mathbf{k}\sigma}, \quad (2)$$

where $a_{\mathbf{k}\sigma}^{\dagger}$ and $b_{\mathbf{k}\sigma}^{\dagger}$ create electrons with spin σ and wavevector \mathbf{k} on sublattices A and B , respectively. The hopping matrix element t is of the order of 2.7eV [6] and $\phi(\mathbf{k}) = \sum_j e^{i\mathbf{k} \cdot \boldsymbol{\delta}_j}$ with $\{\boldsymbol{\delta}_j\}$ the three vectors connecting one site with its nearest neighbors. As a result there are two bands of width $3t$ that touch each

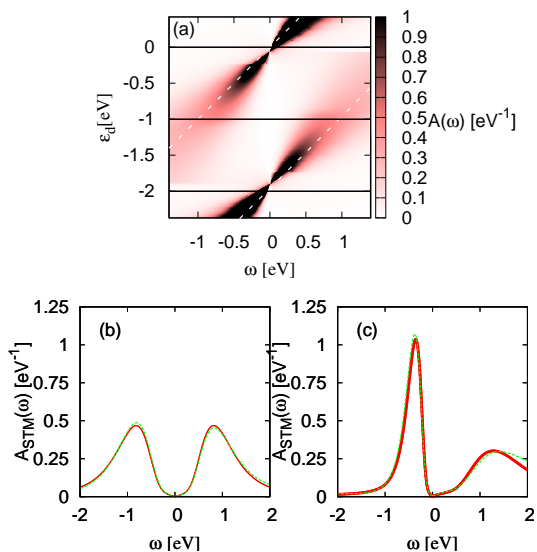


FIG. 1: (Color online) Color map of the spectral density of a magnetic impurity on graphene. Parameters are $U = 2\text{eV}$, $V_{\text{hyb}} = 1\text{eV}$. (b) STM spectra at the impurity for $t_c/t_d = 0$ (solid lines) and $t_c/t_d = 0.3$ (dashed lines). Here $\varepsilon_d = -1\text{eV}$. (c) Same as (b) with $\varepsilon_d = -0.5\text{eV}$ and $t_c/t_d = 0, 1.0$.

other at the corners of the Brillouin zone (Dirac point). Finally, assuming that the impurity is adsorbed on a site of sublattice A , the hybridization Hamiltonian is $H_{\text{hyb}} = \frac{V_{\text{hyb}}}{\sqrt{N}} \sum_{\mathbf{k}\sigma} a_{\mathbf{k}\sigma}^\dagger d_\sigma + d_\sigma^\dagger a_{\mathbf{k}\sigma}$, with N the number of unit cells in the sample.

One of the main ingredients that determines the nature of the solution is the local density of states of the host material. Close to the Dirac point ($E = 0$), the local density of states, per atom and spin, can be approximated by $\rho(E) = \alpha |E|$ with $\alpha = A_{uc}/2\pi\hbar^2 v_F^2$, where A_{uc} is the unit cell area and v_F is the Fermi velocity. In what follows we use this form with a high energy cutoff D . The other relevant parameters (ε_d , U , V_{hyb}) depend on the nature of the impurity, in particular U is of the order of a few eVs for transition metal impurities and smaller for molecules. We solve the problem using the extensions of Wilson's numerical renormalization group (NRG) method that allow to describe a non constant density of states for the host material and to improve the accuracy of the high energy features [15, 17]. We have studied this model numerically for a wide range of parameters. In what follows we will focus on the localized spin regime where the average number of electrons in the impurity level is of the order of one.

In Fig. 1(a) we present a color map of the impurity spectral density $A(\omega)$ for the undoped case— the Fermi energy E_F laying at the Dirac point. The maximums of $A(\omega)$ are shifted from the bare parameters ε_d and $\varepsilon_d + U$ shown in the figure with dashed lines. While for a general $\rho(E)$ some shifts are expected, here the shifts are large

and the energy difference between the peaks is smaller than U . This is due to the interplay between a Hartree correction and the hybridization self-energy [12]. Figs. 1b and 1c show the impurity spectral functions for two different values of ε_d . Note the absence of a Kondo peak at E_F . These spectral densities could be measured with a STM where electrons from the microscope tip tunnel to the impurity sensing the local density of states. If the resonant level is close to the Dirac point ($|\varepsilon_d| \lesssim 1\text{eV}$) the STM can measure the resonance. In general there is some leaking of electrons that tunnel to the substrate generating Fano structures. The STM differential conductance at low temperatures is then given by [18]

$$G(V_b) = \frac{4e^2}{\pi\hbar} \tilde{t}^2 \rho_t A_{STM}(E_F + eV_b), \quad (3)$$

where V_b is the voltage drop from the tip to the sample, and ρ_t is the tip density of states at the Fermi energy. The quantity $A_{STM}(E)$ is the spectral function of the operator $(t_c \psi_\sigma^\dagger + t_d d_\sigma^\dagger)/\tilde{t}$, t_c and t_d are matrix elements for the tunneling of an electron from the tip to the conduction band states and to the impurity orbital, respectively, $\tilde{t} = (t_c^2 + t_d^2)^{1/2}$ and ψ_σ^\dagger is the field operator that creates an electron in a graphene state centered below the tip. In what follows we consider that the tip is on top of the impurity and for simplicity we take $\psi_\sigma^\dagger = N^{-\frac{1}{2}} \sum_{\mathbf{k}\sigma} a_{\mathbf{k}\sigma}^\dagger$. Even for $t_c \simeq t_d$ the effect of t_c is very small due to the smallness of $\rho(E \sim E_F)$, see Fig. 1, and the STM gives direct information of the impurity spectral density.

In the presence of an external magnetic field the impurity is polarized and the spectral densities become spin dependent. In Fig. 2 we present results obtained at low temperatures and low fields. Almost all the weight of the spin-resolved spectral densities is transferred to a single peak at the renormalized energies $\tilde{\varepsilon}_d$ (for the spin up) and $\tilde{\varepsilon}_d + \tilde{U}$ (for the spin down). For the small magnetic field used in the calculation the Zeeman shifts of the peaks are not appreciable. These results suggest that the spin dependent STM differential conductance at high voltages becomes very different for the two spin orientations. To estimate the current of spin- σ electrons, I_σ , we integrate the spin dependent differential conductance. The total current $I = I_\uparrow + I_\downarrow$, in units of $I_0 = 4e\tilde{t}^2 \rho_t / \pi\hbar$, and the current polarization $P_{STM} = (I_\uparrow - I_\downarrow) / I$ are shown in Figs. 2c and 2d, respectively. While the tunneling current I is small, the polarization P_{STM} can exceed 0.98. As we show below the possibility of injecting spin polarized currents is not restricted to the undoped case.

In the case of doped graphene E_F is shifted from the Dirac point. In Fig. 3 we present results for the impurity spectral density $A(\omega)$ at low temperatures. The results show now a Kondo peak at E_F . Following Langreth [19], it can be shown that the spectral density at E_F is given by the usual expression $A(E_F) = \sin^2(\pi\tilde{n}_d/2)/\pi\Gamma$ where \tilde{n}_d is the total charge displaced by the impurity and $\Gamma = \pi\rho(E_F)V_{\text{hyb}}^2$. Our NRG results reproduce well this exact

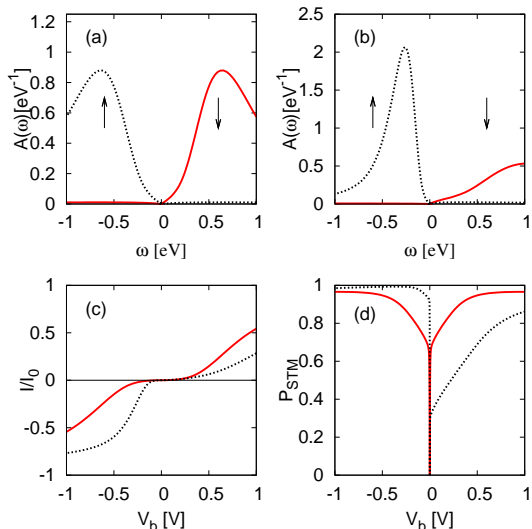


FIG. 2: (Color online) (a) Impurity spectral density for the undoped case in the presence of a small magnetic field $\mu B = 70\mu\text{eV}$ for the spin up (dashed line) and spin down (solid line) projections. Here $V_{\text{hyb}} = 1.4\text{eV}$, $\varepsilon_d = -U/2$ and the other parameters are as in Fig. 1; (b) Same as (a) for $\varepsilon_d = -0.5\text{eV}$; (c) STM current and (d) current polarization as a function of the bias voltage V_b for the spectral densities shown in (a) (solid line) and (b) (dashed line).

result. In Fig. 3c we present results for the impurity charge n_d versus ε_d . The impurity charge changes when the renormalized energies $\tilde{\varepsilon}_d$ and $\tilde{\varepsilon}_d + \tilde{U}$ cross E_F and the plateau corresponding to a localized spin in the impurity, $n_d \sim 1$, is narrowed as V_{hyb} increases. This narrowing should not be interpreted as a reduction of the effective repulsion. As we show below the Kondo temperature is determined by the bare parameter U .

We calculate the impurity spin susceptibility $\chi(T)$, that at low temperatures shows universal behavior, and extract T_K using Wilson's criterion $T_K \chi(T_K)/\mu^2 = 0.025$. The results are shown in Fig. 3d where $\log(T_K)$ as a function of ε_d shows the usual quadratic behavior with a minimum at the center of the $n_d \sim 1$ plateau and a curvature determined by the bare interaction U . For a given set of impurity parameters, T_K varies with doping, or gate voltage, approaching zero for the undoped case.

The transport properties of graphene are peculiar in many aspects and it is interesting to study the effect of adsorbed magnetic impurities. In what follows we present results for the resistivity $\rho_{\text{imp}}(T)$ due to these impurities in the low impurity concentration (c_{imp}) regime. Using the general expression for the conductivity in graphene [20, 21] and evaluating the band propagators in the Born approximation we obtain, to first order in

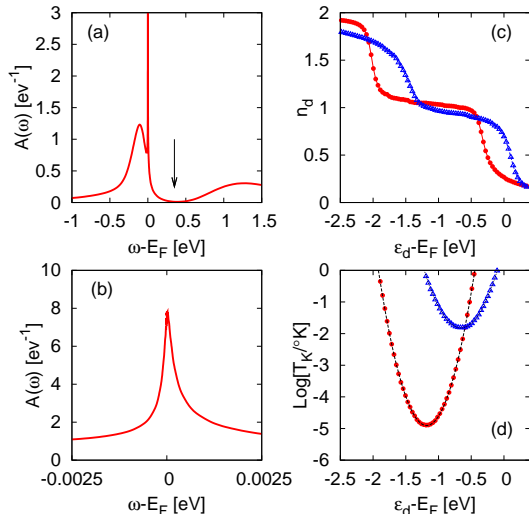


FIG. 3: (Color online) (a) Impurity spectral density for the doped case ($E_F = -0.35\text{eV}$). The arrow indicates the position of the Dirac point. (b) Detail of the Kondo peak. (c) Impurity occupation as a function of the level energy; $V_{\text{hyb}} = 1.4\text{eV}$ and $E_F = -0.35\text{eV}$ (filled circles); $V_{\text{hyb}} = 1.75\text{eV}$ and $E_F = 0.35\text{eV}$ (filled triangles). The local interaction is in both cases $U = 2\text{eV}$. (d) Kondo temperature vs. ε_d for the parameters of (c). The lines are parabolic fits.

c_{imp} ,

$$\rho_{\text{imp}}(T) = \rho_0 V_{\text{hyb}}^2 \left[\int \left(-\frac{\partial f(\omega)}{\partial \omega} \right) \frac{|\omega|}{A(\omega)} d\omega \right]^{-1}, \quad (4)$$

where $\rho_0 = \pi c_{\text{imp}} h/e^2$. The general temperature dependence of the resistivity in the different regimes requires the numerical evaluation of the integral. As shown in Fig. 4, for the undoped case the resistivity is temperature independent while for the doped case we obtain the usual Kondo behavior. The NRG results can be qualitatively reproduced performing some simple approximations. In the undoped case the spin dependent low frequency impurity spectral density is given by $A_\sigma(\omega) \simeq \alpha V_{\text{hyb}}^2 |\omega| [(1-n_{d\sigma})/\varepsilon_d^2 + n_{d\sigma}/(\varepsilon_d + U)^2]$ where $n_{d\sigma}$ is the number of spin σ electrons in the impurity orbital [22]. For the sake of simplicity let's consider first the case $\varepsilon_d = -U/2$ for which $n_{d\sigma} = \frac{1}{2}$, the resistivity is then given by $\rho_{\text{imp}}(T) = \rho_0 \alpha V_{\text{hyb}}^4 / \varepsilon_d^2$. This result corresponds to impurities generating a short range potential of amplitude $\Delta \propto V_{\text{hyb}}^2 / |\varepsilon_d|$. Nevertheless, in the absence of electron-hole symmetry ($\varepsilon_d \neq -U/2$) the system presents a large magnetoresistance due to the difference in the scattering rate of the two spin channels. The contribution of each spin is given by twice the r.h.s. of Eq. (4) with $A(\omega)$ replaced by $A_\sigma(\omega)$, and the total resistivity is

$$\rho_{\text{imp}}(T, B) = \rho_{\text{imp}}(T, B = 0) [1 - \gamma^2 m^2(T, B)], \quad (5)$$

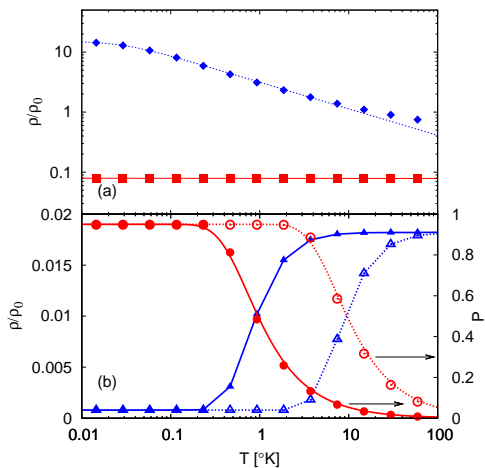


FIG. 4: (Color online) (a) Resistivity vs. temperature for doped ($E_F = -0.35\text{eV}$, solid diamonds) and undoped graphene (solid squares) for $B = 0$, $U = 2\text{eV}$, $V_{\text{hyb}} = 1.4\text{eV}$, and $\varepsilon_d = -0.63\text{eV}$. Doped graphene shows Kondo scaling of the resistivity indicated by the dotted line. (b) Resistivity (triangles) and current polarization (circles) vs. temperature. Undoped graphene, $\mu B = 70\mu\text{eV}$ (solid symbols) and $\mu B = 700\mu\text{eV}$ (open symbols). Other parameters are $U = 3.5\text{eV}$ and $\varepsilon_d = -0.5\text{eV}$.

with $m(T, B) = (n_{d\uparrow} - n_{d\downarrow})$ and for $n_d = 1$, $\gamma = ((\varepsilon_d + U)^2 - \varepsilon_d^2) / ((\varepsilon_d + U)^2 + \varepsilon_d^2)$. The current polarization is $P \equiv (I_{\uparrow} - I_{\downarrow}) / I = \gamma m(T, B)$. These expressions are in good qualitative agreement with the numerical results shown in Fig. 4b. The actual magnetoresistance and the degree of polarization of the current in bulk graphene will depend on the presence and intensity of additional scattering mechanisms. For the magnetoresistance to be observable, the scattering rate due to other mechanisms should be smaller than the one due to the impurities, that is, the impurities should be adsorbed on clean graphene.

For the doped case the Kondo screening in the $T \rightarrow 0$ limit gives

$$\rho_{\text{imp}}(0) = \frac{\hbar}{e^2} \frac{c_{\text{imp}} \sin^2(\pi \tilde{n}_d / 2)}{\pi n}, \quad (6)$$

where n is the number of carriers per carbon atom. In the unitary limit, the resistivity is just determined by the ratio c_{imp}/n . In the limit $T \gg T_K$ we recover the resistivity characteristic of potential scattering defects. The temperature dependence of the resistivity, for $T \lesssim T_K$ shows the universal Kondo behavior [23].

In summary we have numerically solved the problem of a magnetic impurity in graphene and analyzed the effect of external in-plane magnetic fields. We find that as ε_d varies, the region of stability for a localized spin ($n_d \sim 1$) is narrowed and shifted with respect to the $V_{\text{hyb}} \rightarrow 0$ limit, in qualitative agreement with mean field results [12]. Kondo screening of the impurity spin occurs at low temperatures for the doped case. The Kondo

temperature T_K decreases exponentially with decreasing doping and for the undoped case, the impurity behaves as a free spin down to zero temperature. We find very little Fano distortions in the STM spectrum that consequently gives a direct measurement of the impurity spectral densities. Our central results concern the effect of magnetic fields: for zero or low doping, low T_K , the condition $T, T_K < \mu B$ is accessible at moderate values of the external field B . In this regime the impurity spin is polarized and a non-magnetic STM tip can be gated to inject a spin polarized current, that is, the impurity acts as a spin valve. The magnetic field controls the degree and the axis of the spin polarization. In this regime, a finite impurity concentration leads to large magnetotransport effects in bulk graphene: for small values of $|\varepsilon_d - E_F|$ the system shows large magnetoresistance and spin polarized currents. All these effects are unique to graphene: they require $V_{\text{hyb}}^2/|\varepsilon_d|$ to be large and the spin to be free at low temperatures, conditions that are never reached simultaneously in ordinary metals. Our main results are robust even in the presence of defects or other impurities that may change the structure of the pseudogap and the nature of the magnetic screening. However, for magnetic impurities close to one of these defects, new features are expected to appear in the STM spectra that will depend on the nature of the defect.

We acknowledge financial support from ANPCyT Grants No 13829/03, No 483/06 and No 482/06 and CONICET PIP 5254/05.

-
- [1] K. S. Novoselov, A. K. Geim, S. V. Morozov, D. Jiang, Y. Zhang, S. V. Dubonos, I. V. Grigorieva, and A. A. Firsov, *Science* **306**, 666 (2004).
 - [2] K. S. Novoselov, A. K. Geim, S. V. Morozov, D. Jiang, M. I. Katsnelson, I. V. Grigorieva, S. V. Dubonos, and A. A. Firsov, *Nature* **438**, 197 (2005).
 - [3] M. I. Katsnelson, K. S. Novoselov, and A. K. Geim, *Nat. Phys.* **2**, 620 (2006).
 - [4] K. S. Novoselov, Z. Jiang, Y. Zhang, S. V. Morozov, H. L. Stormer, U. Zeitler, J. C. Maan, G. S. Boebinger, P. Kim, and A. K. Geim, *Science* **315**, 1379 (2007).
 - [5] A. K. Geim and K. S. Novoselov, *Nat. Mat.* **6**, 183 (2007).
 - [6] A. H. Castro Neto, F. Guinea, N. M. R. Peres, K. S. Novoselov, and A. K. Geim (2007), arXiv:0709.1163.
 - [7] H. Haugen, D. Huertas-Hernando, and A. Brataas, *Phys. Rev. B* **77**, 115406 (2008).
 - [8] N. Tombros, C. Jozsa, M. Popinciuc, H. T. Jonkman, and B. J. van Wees, *Nature* **448**, 571 (2007).
 - [9] M. Wimmer, İnanç Adagideli, S. Berber, D. Tománek, and K. Richter, *Phys. Rev. Lett.* **100**, 177207 (2008).
 - [10] Y.-W. Son, M. L. Cohen, and S. G. Louie, *Nature* **446**, 347 (2006).
 - [11] B. Dora and P. Thalmeier, *Phys. Rev. B* **76**, 115435 (2007).
 - [12] B. Uchoa, V. N. Kotov, N. M. R. Peres, and A. H. Castro

- Neto, Phys. Rev. Lett. **101**, 026805 (2008).
- [13] K. Sengupta and G. Baskaran, Phys. Rev. B **77**, 045417 (2008).
- [14] D. Withoff and E. Fradkin, Phys. Rev. Lett. **64**, 1835 (1990).
- [15] C. Gonzalez-Buxton and K. Ingersent, Phys. Rev. B **57**, 14254 (1998).
- [16] M. Vojta, Philos. Mag. **86**, 1807 (2006).
- [17] R. Bulla, T. A. Costi, and T. Pruschke, Rev. Mod. Phys. **80**, 395 (2008).
- [18] P. S. Cornaglia and C. A. Balseiro, Phys. Rev. B **67**, 205420 (2003).
- [19] D. C. Langreth, Phys. Rev. **150**, 516 (1966).
- [20] N. M. R. Peres, F. Guinea, and A. H. Castro Neto, Phys. Rev. B **73**, 125411 (2006).
- [21] N. H. Shon and T. Ando, Jour. Phys. Soc. Jpn. **67**, 2421 (1998).
- [22] A. C. Hewson and M. Zuckermann, Phys. Lett. **20**, 219 (1966).
- [23] D. Goldhaber-Gordon, J. Göres, M. A. Kastner, H. Shtrikman, D. Mahalu, and U. Meirav, Phys. Rev. Lett. **81**, 5225 (1998).